

See discussions, stats, and author profiles for this publication at: <https://www.researchgate.net/publication/317724256>

Designing an optimum non-dissipative LC snubber for step-up flyback converters in DCM

Conference Paper · February 2017

DOI: 10.1109/LASCAS.2017.7948040

CITATIONS

4

READS

239

4 authors, including:



[Luciano Garcia](#)

University of Arkansas

19 PUBLICATIONS 91 CITATIONS

[SEE PROFILE](#)



[Alejandro Oliva](#)

National Scientific and Technical Research Council

51 PUBLICATIONS 1,166 CITATIONS

[SEE PROFILE](#)

Some of the authors of this publication are also working on these related projects:



Solid State Transformer [View project](#)



Inductive DC-DC micro-power converters [View project](#)

Designing an Optimum Non-Dissipative LC Snubber for Step-Up Flyback Converters in DCM

Esteban O. Lindstrom
CMNB - INTI,
DIEC -
Universidad Nacional del Sur
Bahía Blanca, Argentina.
estebanl@inti.gob.ar

Luciano A. Garcia-Rodriguez
University of Arkansas
Fayetteville AR, USA.
lgarcia@uark.edu

Alejandro R. Oliva
IIIE, DIEC,
Universidad Nacional del Sur
- CONICET
Bahía Blanca, Argentina.
aoliva@uns.edu.ar

Juan C. Balda
University of Arkansas
Fayetteville AR, USA.
jbalda@uark.edu

Abstract—The optimum design of a non-dissipative LC snubber for step-up flyback converters operating in DCM (Discontinuous Conduction Mode) is presented. Experimental results prove that the optimization of the snubber plays a key role when high efficiency is required. A flat efficiency response larger than 91% along a wide operating range with a peak of 92.2% was accomplished with a transformer having a 6% leakage inductance.

I. INTRODUCTION

The main drawback of the flyback converter is the voltage stress on the switching transistor during its turn off. There is a voltage spike caused by the energy stored in the transformer's leakage inductance taking place every switching cycle. The overvoltage can be reduced by minimizing the leakage inductance; however, this adversely impacts on the cost of the transformer and hence, of the converter. A frequent solution to the overvoltage is the use of snubber circuits that limit the voltage drop across the switch by deriving the excessive energy to an auxiliary circuit.

The various snubber topologies documented in the bibliography can be divided in two main groups: dissipative and non-dissipative snubbers (also called regenerative snubbers). This classification is related to how they process the excessive energy to protect the switch. Those in the first group dissipate the excessive energy [1], [2], reducing the converter's efficiency; while those in the second group return the excessive energy to the source or deliver it to the load [3]–[5]. Therefore, non-dissipative snubbers are preferred over the dissipative ones in terms of energy efficiency.

Dissipative snubbers are further classified in two categories. One that uses clamping devices, such as zener diodes, that become active when the voltage overshoots certain limit, deriving the excessive energy through a low dissipative impedance path. The second category is associated with RC circuits where the excessive energy is first stored in a capacitor and later dissipated in a resistor. Here, the power dissipated in snubbers is related to the leakage inductance of the transformer. Depending on the design, a snubber can dissipate between 1.5 and 6 times the energy stored in the leakage inductor. Thus, if the transformer has a high leakage inductance (around

10% or more) and dissipative snubbers are used, then the maximum achievable efficiency for the converter is limited to 85%, without even considering other losses associated to the converter [6]. In consequence, the use of dissipative snubbers is inadequate for certain applications.

Alternatively, non-dissipative snubbers have the advantage of not degrading so much the converter's efficiency. They are, however, more complex and require more parts. This group of snubbers can also be divided in two subgroups, active and passive. Active non-dissipative snubbers include semiconductor switches and a control loop, parts which make them more expensive [7]–[9]. The passive type only uses capacitors, inductors and diodes; nevertheless, they are usually less efficient [10]–[12], but more reliable. For certain applications the simplicity of the non-dissipative passive snubbers are attractive, especially when the designer does not want to increase the complexity of the controller.

There is a large amount of publications in the literature on snubbers for flyback converters; however, most of them focus on step down converters. Even when the same snubber topology can be used for a step-down or for a step-up flyback converter, its working conditions are different. There is a recent need for step-up flyback converters with high efficiency; to the best of our knowledge, there are just a few recent publications that address this subject [13]–[15] and none of them concentrates on optimizing the snubber's design.

This article focuses on the optimal design of a regenerative snubber for a DCM step-up flyback converter to be used as the maximum power point tracker of a photovoltaic panel. The operating principles of the non-dissipative LC snubber are given in Section II; the proposed design for the snubber is presented in Section III. In Section IV, a case study is designed, measured and compared with other snubber's topology. Finally, the conclusions are given in Section V.

II. OPERATING PRINCIPLES OF THE FLYBACK CONVERTER WITH NON-DISSIPATIVE LC SNUBBER

The schematic diagram of a flyback converter with non-dissipative LC snubber is shown in Fig. 1. The converter itself consists of switch S , the transformer (made with coupled inductors L_1 and L_2 and leakage inductance L_k), rectifier D_o

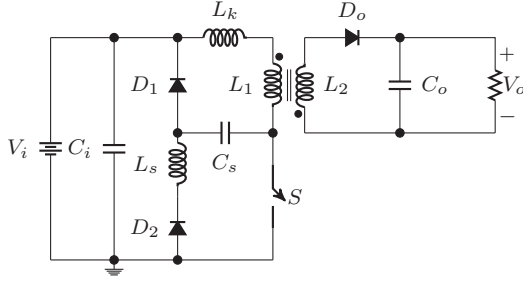


Fig. 1. Flyback converter with non-dissipative snubber.

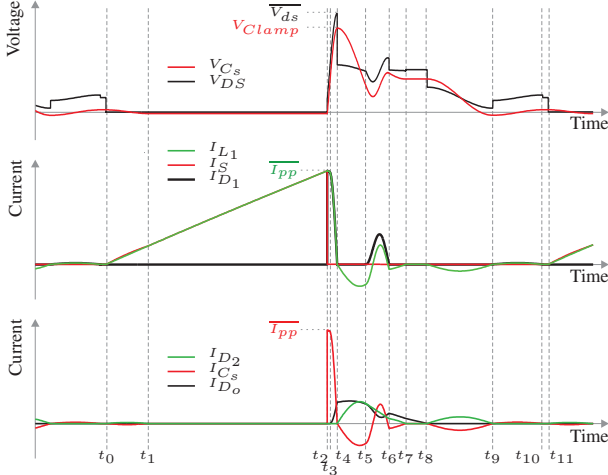


Fig. 2. Typical waveforms of the flyback converter with non-dissipative LC snubber operating under DCM for the maximum duty cycle.

TABLE I
SUMMARY OF OPERATING MODES

	S	D_1	D_2	D_o
Mode I, $t_0 - t_1$	on	off	on	off
Mode II, $t_1 - t_2$	on	off	off	off
Mode III, $t_2 - t_3$	off	on	off	off
Mode IV, $t_3 - t_4$	off	on	off	on
Mode V, $t_4 - t_5$	off	off	on	on
Mode VI, $t_5 - t_6$	off	on	on	on
Mode VII, $t_6 - t_7$	off	off	on	on
Mode VIII, $t_7 - t_8$	off	off	off	on
Mode IX, $t_8 - t_9$	off	off	on	off
Mode X, $t_9 - t_{10}$	off	on	off	off
Mode XI, $t_{10} - t_{11}$	off	off	off	off

and output capacitor C_o . V_i is the voltage source and C_i is the input capacitor. The non-dissipative snubber is made of diodes D_1 and D_2 , inductor L_s and capacitor C_s .

Typical waveforms of the flyback converter with non-dissipative snubber operating under DCM for the maximum duty cycle (worst case in terms of voltage stress across the switch) are shown in Fig. 2, where 11 operating modes can be identified in a switching cycle. The operating modes depend on the states of the semiconductor devices, which are summarized in Table I.

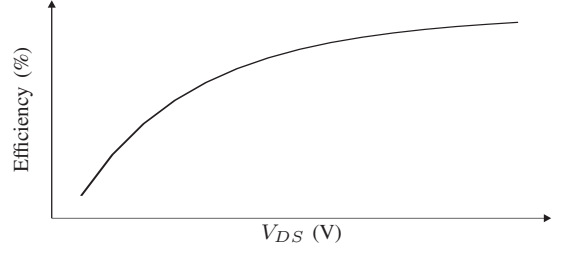


Fig. 3. Efficiency vs. drain-source voltage.

III. DESIGNING THE LC SNUBBER

The design method of the snubber has two goals, one is protecting the switch from the overvoltage stresses produced by the inductances and the other is to optimize the converter's efficiency.

The snubber has to protect the switch at all operating points; doing so for the worst case is sufficient to achieve this task. For this converter topology, the worst case occurs when the maximum energy is stored in L_k , which corresponds to the maximum duty cycle.

Fig. 3 shows a typical curve of efficiency versus drain-source voltage of a flyback converter with a non-dissipative LC snubber. It can be seen that it is convenient to clamp at the highest voltage possible to enhance the efficiency.

The maximum value of V_{DS} , reached during *Mode IV*, depends on the clamping voltage V_{Clamp} and on the input voltage V_i :

$$\overline{V_{DS}} = V_{Clamp} + V_i. \quad (1)$$

V_{Clamp} can be calculated by evaluating KVL along the mesh formed by L_k , L_1 , C_s and D_1 , as

$$V_{Clamp} = V_o \frac{N_p}{N_s} + \sqrt{\frac{L_k \overline{I_{pp}}^2}{C_s}}, \quad (2)$$

where $\overline{I_{pp}}$ is the maximum current of the primary winding.

Finally, solving (2) for C_s yields the capacitance that produces the maximum efficiency out of the converter

$$C_s = \frac{L_k \overline{I_{pp}}^2}{\left(\overline{V_{DS}} - V_i - V_o \frac{N_p}{N_s} \right)^2}. \quad (3)$$

Notice that (3) only depends on the flyback converter parameters and the maximum value of V_{DS} , making the design of C_s fairly simple.

The snubber inductor has two functions; namely, it helps returning to V_i the energy stored in C_s and also limits the peak current of the main switch during the polarity inversion of the voltage across C_s in *Mode I*. This sets the limits of possible values for the inductance.

The upper limit is imposed for the proper snubber functionality. In *Mode I*, during the on time of the switch, the polarity of the voltage drop across capacitor C_s needs to be inverted through the tank circuit formed with L_s . The voltage inversion takes half of the resonant period; therefore, this half

TABLE II
PARAMETERS OF THE EXPERIMENTAL FLYBACK CONVERTER

V_i	V_o	f_s	\overline{D}^1	\underline{D}^1	$V_{B_{sw}}^2$	$\overline{I_{sw}}$	P
25 V	200 V	84 kHz	0.5	0.1	200 V	144 A	84 W

¹ \overline{D} and \underline{D} are duty cycle maximum and minimum, respectively.

² $V_{B_{sw}}$ is the switch's breakdown voltage.

TABLE III
PARAMETERS OF THE EXPERIMENTAL FLYBACK TRANSFORMER

L_1	L_2	L_k	N_p	N_s	R_1^1	R_2^1
10 μ H	160 μ H	0.6 μ H	1	4	150 m Ω	300 m Ω

¹ R_1 and R_2 are the parasitic resistance of the primary and secondary winding, respectively.

period must be shorter than the minimum on time to ensure the voltage inversion. The upper limit for the inductance can be calculated as

$$L_s < \left(\frac{\underline{D}}{f_s \pi} \right)^2 \frac{1}{C_s}. \quad (4)$$

The lower limit is given by (5), and it is set by the maximum peak current allowed by the switch, $\overline{I_{sw}}$:

$$L_s > \frac{\overline{I_{sw}}^2 - \sqrt{\overline{I_{sw}}^4 - \left(\frac{\pi V_i^2 C_s}{L_k + L_1} \right)^2}}{\frac{C_s}{2} \left(\frac{\pi V_i}{L_1 + L_k} \right)^2}. \quad (5)$$

IV. CASE STUDY

The snubber design, simulation and experimental results that validate the optimum design are presented in this section. Table II summarizes the parameters of the flyback converter, for which the snubber is designed, and the maximum ratings of the switch, $V_{B_{sw}}$ and $\overline{I_{sw}}$. The parameters of the transformer are shown in Table III, where R_1 and R_2 are the parasitic resistances of the primary and secondary windings, respectively. It is worth noting that the leakage inductance of the transformer is high (6%). This implies a reduction of the converter's cost because transformers with high leakage inductance are generally less expensive.

Snubber Design

The design procedure starts by calculating C_s using (3), that gives $C_s = 8.22$ nF for $\overline{V_{DS}} = 190$ V. Using the calculated C_s in (4) and (5), the limit values for L_s are obtained as $778 \text{ pH} < L_s < 17.4 \text{ } \mu\text{H}$. The experimental prototype was constructed using commercial values for $C_s = 8.22$ nF and $L_s = 8.2 \text{ } \mu\text{H}$.

Waveforms

Fig. 4 shows the simulated and measured waveforms on the same graph for easy comparison. It can be seen that the snubber works correctly, clamping voltage V_{ds} to 196 V. In general, the experimental and simulated waveforms are similar. There are, however, three clear differences between the experimental and simulated data: the voltage drop across

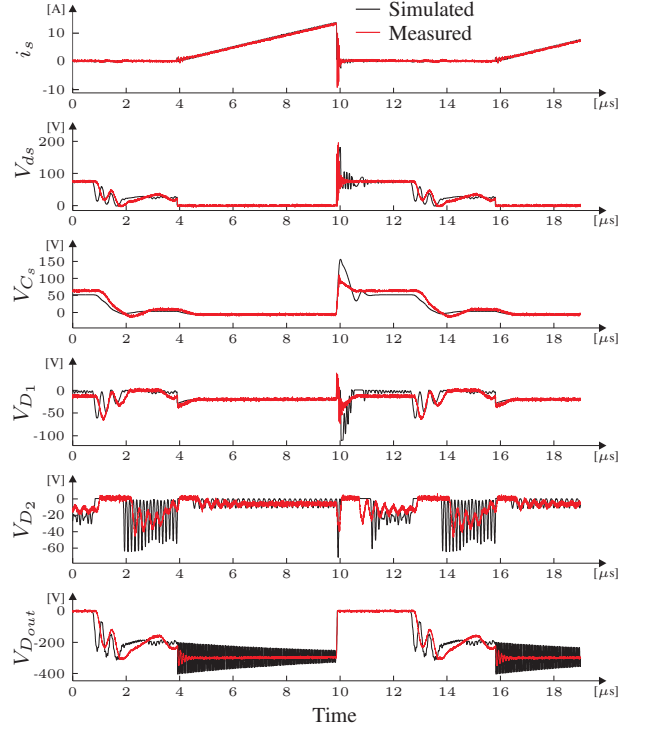


Fig. 4. Simulated and measured waveforms.

the snubber capacitor, V_{C_s} , has a smaller peak amplitude, *Modes VI* and *VII* are not present and the high frequency oscillations are attenuated.

Voltage V_{C_s} does not reach the expected peak, mainly because of the damping action of the parasitic resistors in the path $L_1 - L_k - C_s - D_1$ and high current peaks involved that produce high voltage drops. Additionally, the printed circuit board's (PCB) parasitic inductors force V_{ds} to exceed its design limit of 190 V and also to reduce the voltage across C_s . Special care must be taken when designing the PCB to reduce these parasitic elements.

A close look at V_{ds} , between 10 and 12 μ s, reveals the absence of two operating modes; this is also evident because V_{D1} does not reach zero. Part of the energy captured by the snubber is dissipated by the parasitic elements of the snubber and the PCB; thus, D_1 never turns on and the snubber evolves from *Mode V* to *Mode VII* without going through the intermediate modes. The high frequency oscillations present in the simulations appear attenuated in the experimental measurements; again, the parasitic resistors are responsible for this. Even when the simulations were performed with realistic component models, not all the parasitics were considered.

Efficiency

The method for selecting C_s is validated through the experimental results. It is shown in Fig. 5, where it can be noticed that as the capacitance deviates from the optimum value (the smallest value that guarantees that the switch is protected) the efficiency decreases. The efficiency was measured for different

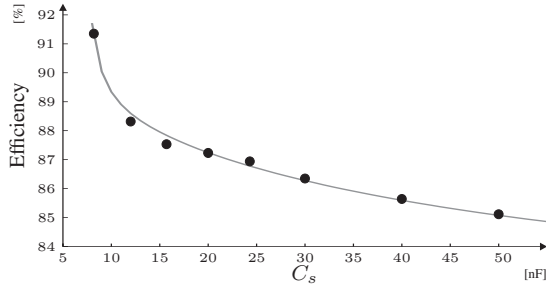


Fig. 5. Efficiency vs. C_s capacitance.

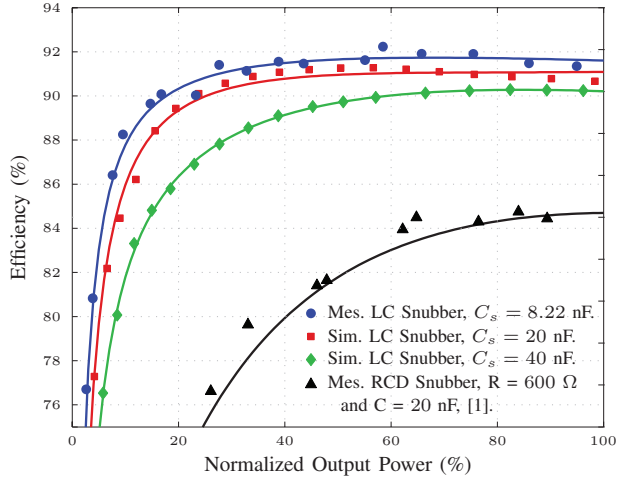


Fig. 6. Efficiency vs. normalized output power for the proposed non-dissipative LC snubber, two sub-optimized non-dissipative LC snubbers and RCD snubber.

values of C_s , where D , V_i and V_o were kept constants at 50%, 25 V and 200 V, respectively.

Fig. 6 compares the efficiency of the same converter equipped with four different snubbers: one optimized as proposed in this article (●), two suboptimal LC snubbers (■ - ◆) and an RCD snubber (▲). The (●) and (▲) curves were obtained experimentally, while the (■) and (◆) are the result of computer simulations. The suboptimal snubbers were built using 20 nF and 40 nF for C_s . All curves account for the controller and driver losses. It can be noticed that as C_s approaches the optimum value the efficiency increases while the curve flattens. When the snubber capacitor increases beyond the optimum, more energy recirculates; thus part of it is dissipated before reaching the load and the efficiency gets reduced. In this example any of the considered LC snubbers outperform the RCD snubber. The efficiencies obtained by simulation (Fig. 6) are higher than the experimental values (Fig. 5) because not all the parasitics were considered for simulation.

V. CONCLUSIONS

It has been shown that by following the design guidelines the efficiency is maximized. In addition, the LC snubber does not have a negative impact on the turn-on stress of the switch, since most of the energy captured by the snubber is returned in previous intermediate modes.

The flyback converter with the optimized LC snubber design proposed in this article has a flat efficiency curve with an efficiency larger than 91% in a wide range included between 30% and 100% of the maximum power, a desired characteristic in photovoltaic applications. The peak efficiency of 92.2% was obtained at 61.6% of the maximum power.

The LC snubber optimization process considerably improves the converter's performance without adding any extra cost, as can be seen in Fig. 5. The optimum LC snubber design proposed in this paper is a good alternative for the design of step-up flyback converters used as the dc-dc stage of microinverters; it does not increase the cost, keeps a low part count impacting positively on the reliability, provides a flat efficiency curve over a wide power range and reduces the current stress at the turn on.

REFERENCES

- [1] P. Meng, X. Wu, J. Yang, H. Chen, and Z. Qian, "Analysis and design considerations for EMI and losses of RCD snubber in flyback converter," in *Proc. of the Twenty-Fifth Annual IEEE Applied Power Electronics Conf. and Exposition (APEC)*, Feb. 2010, pp. 642–647.
- [2] P. Meng, H. Chen, S. Zheng, X. Wu, and Z. Qian, "Optimal design for the damping resistor in RCD-R snubber to suppress common-mode noise," in *Proc. of the Twenty-Fifth Annual IEEE Applied Power Electronics Conf. and Exposition (APEC)*, Feb. 2010, pp. 691–695.
- [3] R. Petkov and L. Hobson, "Analysis and optimisation of a flyback converter with a nondissipative snubber," in *Proc. of the IEEE Electric Power Applications*, vol. 142, no. 1, Jan. 1995, pp. 35–42.
- [4] A. Abramovitz, T. Cheng, and K. Smedley, "Analysis and design of forward converter with energy regenerative snubber," *IEEE Trans. Power Electron.*, vol. 25, no. 3, pp. 667–676, Mar. 2010.
- [5] G. Jun-yin, W. Hong-fei, C. Guo-cheng, and X. Yan, "Research on photovoltaic grid-connected inverter based on soft-switching interleaved flyback converter," in *Proc. of the 5th IEEE Conf. on Industrial Electronics and Applications (ICIEA)*, Jun. 2010, pp. 1209–1214.
- [6] R. Kollman. (2010) Snubbing the flyback converter. [Online]. Available: http://www.eetimes.com/document.asp?doc_id=1273320.
- [7] B. Akin, "An improved ZVT-ZCT PWM DC-DC boost converter with increased efficiency," *IEEE Trans. Power Electron.*, vol. 29, no. 4, pp. 1919–1926, Apr. 2014.
- [8] L. Chen, H. Hu, Q. Zhang, A. Amirahmadi, and I. Batarseh, "A boundary-mode forward-flyback converter with an efficient active LC snubber circuit," *IEEE Trans. Power Electron.*, vol. 29, no. 6, pp. 2944–2958, Jun. 2014.
- [9] M. A. Rezaei, K. J. Lee, and A. Q. Huang, "A high-efficiency flyback micro-inverter with a new adaptive snubber for photovoltaic applications," *IEEE Trans. Power Electron.*, vol. 31, no. 1, pp. 318–327, Jan. 2016.
- [10] A. Abramovitz, C.-S. Liao, and K. Smedley, "State-plane analysis of regenerative snubber for flyback converters," *IEEE Trans. Power Electron.*, vol. 28, no. 11, pp. 5323–5332, Nov. 2013.
- [11] M. Mohammadi and M. Ordonez, "Flyback lossless passive snubber," in *Proc. of the IEEE Energy Conversion Congress and Exposition (ECCE)*, Sep. 2015, pp. 5896–5901.
- [12] S. W. Lee and H. L. Do, "A single-switch AC-DC LED driver based on a boost-flyback pfc converter with lossless snubber," *IEEE Trans. Power Electron.*, vol. PP, no. 99, p. 1, 2016.
- [13] C. Vartak, A. Abramovitz, and K. Smedley, "Analysis and design of energy regenerative snubber for transformer isolated converters," *IEEE Trans. Power Electron.*, vol. 29, no. 11, pp. 6030–6040, Nov. 2014.
- [14] J.-H. Lee, T.-J. Liang, and J.-F. Chen, "Isolated coupled-inductor-integrated DC-DC converter with nondissipative snubber for solar energy applications," *IEEE Trans. Ind. Electron.*, vol. 61, no. 7, pp. 3337–3348, Jul. 2014.
- [15] D. D. Kumar and K. Maheswaram, "High step-up forward flyback converter with nondissipative snubber for solar energy application," *International Journal of Advanced Research in Electrical, Electronics and Instrumentation Engineering*, vol. 4, no. 7, pp. 6345–6351, Jul. 2015.